

SPECTROSCOPIC, THERMAL ANALYSES, XRD SPECTRA AND NEMATOCIDAL ACTIVITY STUDY OF SOME NEW N₂O₂ TETRADENTATE SCHIFF BASE METAL IONS COMPLEXES

Mohamed S. El-attar^{1*}, Sadeek A. Sadeek¹, Ahmed F. El-Farargy¹,
Nosa S. Abd El-Lattif² and Sherif M. Abd El-Hamid³

¹Department of Chemistry, Faculty of Science, Zagazig University, Zagazig, Egypt

²Department of Pesticides Formulation, Central Agricultural Pesticides Laboratory, Cairo, Egypt

³Department of Basic Science, Higher Future Institute of Engineering and Technology,
Mansoura, Egypt

(Received February 18, 2021; Revised October 5, 2021; Accepted October 5, 2021)

ABSTRACT. A series of metal complexes [Co(HL)₂(H₂O)₂]Cl₂.5H₂O (**A**), [Cu(HL)₂](CH₃COO)₂.2H₂O (**B**), [Y(HL)₂]Cl₃.2H₂O (**C**), [ZrO(HL)₂H₂O]Cl₂.H₂O (**D**), [La(HL)₂(H₂O)₂]Cl₃.5H₂O (**E**) and [UO₂(HL)₂](CH₃COO)₂ (**F**) were prepared. The structures of the compounds in solid state were detected by micro analytical, Fourier transform IR, ¹H NMR, UV-Vis, mass, X-ray diffraction spectra, molar conductivity, magnetic susceptibility measurements and TG/DTG analysis. The IR spectral data point out that the ligand behaves as tridentate in nature with Cu(II), Y(III), U(VI) and bidentate with Co(II), Zr(IV) and La(III) metal ions. The conductivity values showed that the complexes found as electrolytes and the XRD models of the complexes indicated crystalline nature. The thermodynamic parameters of compounds have been detected using Coats-Redfern and Horowitz-Metzger methods at n = 1 and n = 1 and values point out more ordered activated complex formation. The nematocidal efficacy of compounds was assessed.

KEY WORDS: Schiff base, Spectroscopic analysis, Thermal analysis, XRD, Nematicidal

INTRODUCTION

Among the root-knot nematodes, *Medioilgyne javanica*, *Meloidogyne incognita*, *Meloidogyne arenaria* and *Meloidogyne hapla*, are of major agronomic importance, being responsible for at least 90% of all damage caused by these nematode [1-3]. In Egypt root-knot nematodes, *Meloidogyne javanica*, is becoming an actual threat to around all vegetable crops and have been deemed as restricting factors in crop production [4, 5]. In the great intensively grown crops, artificial nematicides are one of the primary means of control. However, with continued use their efficiency can decline and there are concerns of the impact that these chemicals have on the environment. Many compounds have now been dragged out from use promoting the need for new safe and effective options [6, 7]. Schiff bases are the most immensely utilized organic compounds comprising a carbon-nitrogen double bond as functional group [8, 9]. Schiff bases of aliphatic aldehydes are comparatively unstable and easily polymerizable than aromatic aldehyde [10, 11]. Schiff base ligands have interesting ligation properties due to the presence of distinct coordination sites and these ligands are able to coordinate with many various metals and they easily form stable complexes [12, 13]. Schiff base and its complexes have important biological application such as antimicrobial, antitumor, antioxidant, anti HIV, antiviral, antiallergenic and nematicidal and also play an essential role in agriculture, pharmaceutical and industrial chemistry [14-17]. In this study, the metal complexes of ethyl 2-(2-hydroxybenzylidene)-hydrazine carboxylate (HL) with Co(II), Cu(II), Y(III), Zr(IV), La(III) and U(VI) have been synthesized and characterized using melting point, elemental analysis, molar conductivity, infrared, UV-Vis, proton NMR, mass spectra, thermal analysis as well as XRD to

*Corresponding author. E-mail: myelattar@yahoo.com

This work is licensed under the Creative Commons Attribution 4.0 International License

interpret their chemical stability and thermodynamic parameters have been calculated from thermal analyses. The nematocidal activity of the investigated complexes and free ligand were evaluated.

EXPERIMENTAL

Materials and reagents

All chemicals used for the synthesis of compounds were of the analytical reagent grade, commercially available from various sources and highest purity ready-made. Salicylaldehyde, absolute ethanol, toluene, $\text{FeCl}_3 \cdot 6\text{H}_2\text{O}$, $\text{ZrOCl}_2 \cdot 8\text{H}_2\text{O}$ (99.9%), and AgNO_3 were purchased from Fluka chemical Co. $\text{CoCl}_2 \cdot 6\text{H}_2\text{O}$, $\text{Cu}(\text{CH}_3\text{COO})_2$, $\text{YCl}_3 \cdot 6\text{H}_2\text{O}$, $\text{LaCl}_3 \cdot 7\text{H}_2\text{O}$ and $\text{UO}_2(\text{CH}_3\text{COO})_2 \cdot 2\text{H}_2\text{O}$ were purchased from Aldrich Chemical Co. Organic compound ethylcarbazate was purchased from Obour Pharmaceutical Industrial Company.

Preparation of ethyl 2-(2-hydroxybenzylidene)-hydrazine carboxylate Schiff base ($\text{C}_{10}\text{H}_{12}\text{N}_2\text{O}_3$) HL

The Schiff base was synthesized by mixing an ethanolic solution of ethylcarbazate 1 mmol (0.104 g) with salicylaldehyde 1 mmol (0.122 mL) into round bottomed flask equipped with a magnetic stirrer. The contents in the flask were boiled under reflux for 10 h. the resulting solution was concentrated to 8 mL on a water bath. Upon cooling at 0 °C white precipitate obtained was filtered off, washed several times with ethanol and dried under vacuum over fused CaCl_2 .

Preparation of complexes

The pink solid complex (**A**) was prepared by adding 1 mmol (0.238 g) of cobalt chloride hexahydrate in 30 mL absolute ethanol was added drop wise to a stirred solution 1 mmol (0.208 g) of HL in 30 mL ethanol. The reaction mixture was boiled and stirred under reflux for 12 h. The pink precipitate obtained was filtered, washed several times with ethanol and dried under vacuum over fused CaCl_2 . The dark green, oily, light yellow, beige and red solid complexes of (**B**), (**C**), (**D**), (**E**) and (**F**) were prepared in a similar manner described above by using ethanol as solvent. Complex (**A**): bis[ethyl-2-(2-hydroxybenzylidene)-hydrazine-carboxylate] diaqua cobalt chloride pentahydrate. Complex (**B**): bis[ethyl-2-(2-hydroxybenzylidene)-hydrazine-carboxylate] cupper acetate dihydrate. Complex (**C**): bis[ethyl-2-(2-hydroxybenzylidene)-hydrazine-carboxylate] yttrium chloride dihydrate. Complex (**D**): bis[ethyl-2-(2-hydroxybenzylidene)-hydrazine-carboxylate] aqua oxo zirconium chloride monohydrate. Complex (**E**): bis[ethyl-2-(2-hydroxybenzylidene)-hydrazine-carboxylate] diaqua lanthanum chloride pentahydrate. Complex (**F**): bis[ethyl-2-(2-hydroxybenzylidene)-hydrazine-carboxylate] dioxo uranyl acetate.

Instruments

Carbon, hydrogen and nitrogen contents were determined on a Perkin Elmer CHN 2400. The percent of the metal ions were identified gravimetrically by conversion of the solid products into metal oxide and also identified by using atomic absorption method. Spectrometer model PYE-UNICAM SP 1900 supplied with the corresponding lamp was used for this purposed. Fourier transform-IR spectra in KBr discs were registered in the range from 4000-400 cm^{-1} with FT-IR 460 PLUS Spectrophotometer, proton NMR spectra were registered on Varian Mercury VX-300 NMR Spectrometer using dimethyl sulfoxide- d_6 as solvent. TG-DTG measurements were done

under N₂ atmosphere within the temperature range from room temperature to 1000 °C using TGA-50H Shimadzu, the mass of sample was accurately weighted out in an aluminum crucible. Electronic spectra were done using UV-3101PC Shimadzu. The absorption spectra were recorded as solutions in DMSO-d₆ using UV-3101PC Shimadzu. Mass spectra were recorded on GCMS-QP-1000 EX Shimadzu (ESI-70 eV) in the range from 0-1090. XRD powder analyses were set by using a Philips Analytical X-ray BV, diffractometer type PW 1840. Radiation was provided by a copper target (Cu anode 2,000 W) high intensity X-ray tube hold at 40 kV and 25 mA. Magnetic susceptibilities of the samples were carried out on a Sherwood scientific magnetic balance using Gouy balance at room temperature using mercury(II) tetrathiocyanatocobaltate(II) as calibrant. The molar conductance of 1×10⁻³ M solutions of the ligand and its complexes in dimethylformamide was estimated at room temperature using CONSORT K410. Melting points were registered by a Buchi apparatus. All measurements were done with new prepared solutions at room temperature.

Nematicidal investigation

Nematicidal activity of the ligand and its metal complexes was inspected [18]. Root-Knot nematode (*Meloidogyne javanica*) propagated in pure culture in central agricultural pesticides laboratory. Individual egg-masses with their mature females were removed from galls of the infected roots. Each egg-mass was located in 10 ml glass capsule containing distilled water. The female under the particular egg-mass was removed from root tissue, dissected and identified by microscope examination of its perineal pattern system. Identification was recorded according to its corresponding egg-mass of previously identified females. Egg-mass were singly put on root system of two weeks old tomato seedling race number (CV). Pritchard in 15 cm clay pots filled with steam sterilized sandy loam soil. The inoculated pots were watered thoroughly and preserved in greenhouse at 25±5 °C. Two months after inoculation the plants were removed from the pots and the root system of each plant was examined for nematodes infection and reproduction. Samples were from the infected roots which contained adult females and egg-masses for identification to confirm the nematode species to their original patterns. The infected roots were used for inoculation of tomato seed lings CV. Pritchard growth in 25 cm pots filled with 3:1 mixture of sandy: clay soil. New tomato seedlings were transplanted to the pots as needed. By repeating this procedure enough quantities of inocula from pure culture were obtained.

Bioassay technique

Evaluation of tested ligand and its complexes as nematicides were carried out according to migration method [18]. Bioassay unit consists of polyethylene tube of 1.3 cm long and 2.4 cm diameter covered at one end with two layers, the first one is paper handkerchief then muslin cloth. It filled with washed air-dried sand of particle size 250 µm and placed upright in a Petri-dish 5 cm diameter serial concentration from tested ligand and its complexes were prepared in ethanol. 1 mL of tested concentration was pipetted on surface of sand in each tube and kept at 25±5 °C to evaporate the solvent. After 24 h, 1 mL of water was pipetted on roof of sand in each tube, then 1 mL of nematode suspension containing 100 second stage larvae of *M. javanica* was pipetted on the roof of the sand in each tube. Each bioassay unit was transferred to petri dish (9 cm diam) containing filter paper saturated with 2 mL water to serve as humidity room to prevent evaporation. After 24 h the bioassay unit took up from humidity room and 8 mL distilled water was added in Petri dish of bioassay unit. The number of second stage larvae that had migrated in bioassay dish was recorded 72 h later. The number of migrated second stage larvae in treatments was expressed as percentage of number in control and each treatment was repeated four times. The percentages of inhibition were confirmed.

RESULTS AND DISCUSSION

All the synthesized compounds are colored, stable at room temperature, non-hygroscopic, insoluble in water and partially soluble in organic solvents, for example CHCl_3 , but soluble in dimethylformamide and dimethyl sulfoxide. The analytical data of the compounds along with some physical characteristics are summarized in Table 1. The Schiff base HL reacts with Co(II), Cu(II), Y(III), Zr(IV), La(III) and U(VI) ions in absolute ethanol to form stable solid complexes. The complexes are stable at room temperature. The complexes were acquired as colored powdered materials and characterized using elemental analyses, magnetic susceptibility, melting point, X-Ray Diffraction, infrared, mass, UV-Vis, proton NMR spectra and thermal analyses. The molar ratio for all synthesized complexes is HL:M = 1:1 which was established from the results of the chemical analyses. Also, all the prepared complexes hold water molecules except complex (F) and the number of bound water molecules being different. The elemental analyses agree with the chemical formulas of compounds. The spectroscopic data such as (IR and thermal analysis) prove that the presence of water in the composition of the complexes. The metal ions are coordinated with oxygen (phenolic, carbonyl) and nitrogen atoms of HL to forming five and six membered rings and complete the coordination number with one or two water molecules. The molar conductance values of HL and its metal complexes in DMF with standard reference, using 1×10^{-3} M solutions at room temperature were found to be in the range 15.00 to 273.2 $\text{S cm}^2 \text{mol}^{-1}$ (Table 1). The complexes solutions were tested with aqueous solutions of AgNO_3 and FeCl_3 , a white precipitate and red brownish color were formed which indicated the presence of Cl^- and $(\text{CH}_3\text{COO})^-$ as counter ions [19, 20]. Qualitative reactions also agree well with the molar conductance data. The nematocidal activity of the compounds was also evaluated.

Table 1. Elemental analysis and physico-analytical data for HL and its metal complexes.

Compounds M.Wt. (MF)	Color (yield) %	M.P. (°C)	% found (calcd)					S cm^2 mol^{-1}
			C	H	N	Cl	M	
HL 208.21 ($\text{C}_{10}\text{H}_{12}\text{N}_2\text{O}_3$)	White (90)	138	57.65 (57.68)	5.73 (5.81)	13.43 (13.45)	-	-	15.00
(A) 672.37 ($\text{CoC}_{20}\text{H}_{38}\text{N}_4\text{Cl}_2\text{O}_{13}$)	Pink (80)	198	35.69 (35.73)	5.02 (5.70)	8.29 (8.33)	10.50 (10.55)	8.73 (8.76)	190.1
(B) 634.09 ($\text{CuC}_{24}\text{H}_{34}\text{N}_4\text{O}_{12}$)	Dark Green (70)	>300	45.43 (45.46)	5.33 (5.40)	8.80 (8.84)	-	10.00 (10.02)	161.1
(C) 647.72 ($\text{YC}_{20}\text{H}_{28}\text{N}_4$ Cl_3O_8)	Oily (75)	120	37.02 (37.08)	4.29 (4.36)	8.61 (8.65)	16.42 (16.42)	13.69 (13.73)	273.2
(D) 630.59 ($\text{ZrC}_{20}\text{H}_{28}\text{N}_4\text{Cl}_2\text{O}_9$)	Light Yellow (80)	>300	38.03 (38.09)	4.40 (4.48)	8.86 (8.88)	11.23 (11.24)	14.40 (14.47)	189.2
(E) 787.80 ($\text{LaC}_{20}\text{H}_{38}\text{N}_4$ Cl_3O_{13})	Beige (70)	118	30.44 (30.49)	4.80 (4.86)	7.09 (7.11)	13.49 (13.50)	17.60 (17.63)	269.2
(F) 804.54 ($\text{UC}_{24}\text{H}_{30}\text{N}_4\text{O}_{12}$)	Red (75)	>300	35.78 (35.83)	3.70 (3.76)	6.93 (6.96)	-	29.56 (29.59)	160.0

IR absorption spectra

The infrared spectra of HL and its metal complexes could be taken as a diagnostic of the mode of the coordination of the ligand to the metal ions (Table 2). The free ligand and its complexes

have major peaks in the range 3386-3442 and 3240-3244 cm⁻¹ in medium appearance assigned to O-H and N-H stretching [21, 22]. However, very strong and strong bands at 1714 and 1621 cm⁻¹ are assigned to C=O and C=N group. As expected, in complexes (B), (C) and (F) the shift of (OH), (C=O) and (C=N) to lower or higher frequency, this indicate that HL act as neutral tridentate [23, 24]. Here, metal ions react with tridentate Schiff base forming complexes of monomeric structures (Scheme 1), where the ligand forming six and five membered rings [25]. But in case of complexes (A), (D) and (E) the shift of (O-H) and (C=N) to a lower wave number indicate coordination occur through oxygen of phenolic group and nitrogen atom in C=N group with the central metal ions [26, 27] and the ligand acts as neutral bidentate forming six membered ring. The spectra of the isolated solid complexes showed a group of bands with different intensities which characteristics for (M-O) and (M-N). The (M-O) and (M-N) bands observed at 658, 589 and 472 cm⁻¹ for complex (A), 676, 599, 551, 513 and 483 cm⁻¹ for complex (B), at 656, 602, 517 and 472 cm⁻¹ for complex (C), at 654, 592 and 469 cm⁻¹ for complex (D), at 657, 589, 518 and 472 cm⁻¹ for complex (E) and 648, 605, 531 and 494 cm⁻¹ for complex (F) which are absent in the spectrum of free HL. Therefore, it is concluded that all the IR data suggested that the metal was bonded to the Schiff bases through the phenolic oxygen and the C=N nitrogen [28, 29] and oxygen of carbonyl group involved in the coordination sphere, therefore HL behave as tridentate ligand. The data showed that (Zr=O) is a medium band at 887 cm⁻¹ and the _{as}(U=O) and _s(U=O) absorption bands occurs as very strong at 901 and medium at 830 cm⁻¹, respectively [30, 31]. The (U=O) of the uranyl unit in the complex (F) occurs at lower frequency values parallel to those for the same unit, UO₂, in simple salt. The _s(U=O) value was used to calculate both the bond length and the bond stretching force constant, F(U=O), for UO₂ bond in our complex [32-34]. The calculated bond length and force constant values are 1.744 Å and 666.49 Nm⁻¹. Comparing between the calculated values for F_{U=O}, for U=O bond length in my complex [UO₂(HL)₂](CH₃COO)₂, it seems that the HL have pronounced effect on these values.

Table 2. Selected infrared absorption frequencies (cm⁻¹) and tentative assignments for HL and its metal complexes.

Compounds	(O-H); phenolic and H ₂ O;	(N-H) stretching	(C=O)	(C=N)	(Zr=O), _{as} (U=O) _s (U=O)	(M-O), (M-N)
HL	3442mbr	3241vs	1714vs	1621s	-	-
(A)	3404mbr	3240s	1713vs	1550vs	-	658w, 589s, 472s
(B)	3386mbr	3243w	1703s	1610vs	-	676m, 599ms, 551m, 513m, 483w
(C)	3390mbr	3241s	1724vs	1547vs	-	656m, 602ms, 517w, 472ms
(D)	3400br	3240ms	1715vs	1549s	887w	654w, 592w, 469w
(E)	3410mbr	3243m	1714s	1550ms		657w, 589s, 518vw, 472w
(F)	3421mbr	3244m	1656s	1560vs	901vs, 830m	648ms, 605ms, 531m, 494m

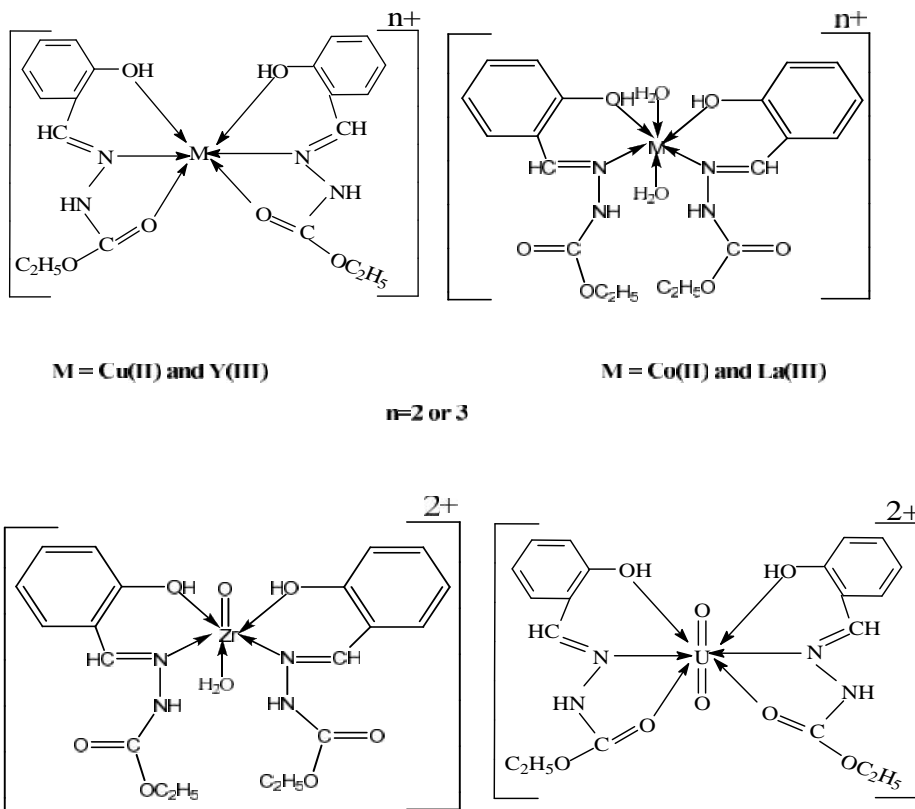
Keys: s = strong, w = weak, v = very, m = medium, br = broad, = stretching.

$$M_O = \text{mass of oxygen} \quad \nu = \frac{1}{2} \pi c \sqrt{F/M_O} \quad (1)$$

$$r(U = O) = \frac{1.08}{\sqrt[3]{F}} + 1.17 \quad (2)$$

Or

$$r(U - O) = 1.993 F^{-1/3} + 0.66 \quad (3)$$



Scheme 1. The coordination mode of Co(II), Cu(II), Y(III), Zr(IV), La(III) and U(VI) with HL.

Magnetic measurements and electronic spectra

The magnetic moments (as B.M.) of the complexes were measured at room temperature. The complexes (A) and (B) are found in paramagnetism with measured magnetic moment values at 1.80 and 2.25 B.M. The room temperature values typify the existence of octahedral configuration in low spin state. The other complexes of (C), (D), (E) and (F) were found as diamagnetism. The formation of the metal complexes was also confirmed by UV-Vis spectra. Absorption measurements based upon ultraviolet and visible radiation find widespread application for the identification and determination of inorganic and organic species. The absorption spectra of the free HL and its metal complexes were recorded in the wavelength interval from 200 to 800 nm (Table 3). It can be seen that free HL absorbed at 275, 284 and 318

nm. The bands at 275 and 284 nm may be attributed to $n \rightarrow \pi^*$ transition and the band observed at 318 nm are assigned to $\pi \rightarrow \pi^*$ transitions. The shift of bands to higher (bathochromic shift) or lower (hypsochromic shift) values upon complexation indicate that the formation of their metal complexes. The complexes show a group of new bands at 572, 563, 500, 527, 509 and 536 nm which may be assigned to ligand to metal charge-transfer [35, 36]. The d-d transition absorption spectra for complexes (A) and (B) showed one absorption band at 609 and 618 nm which are assigned to ${}^4T_{1g}(F) \rightarrow {}^4T_{1g}(P)$ and ${}^2B_1 \rightarrow {}^2E_g$ transitions in favor of octahedral geometry [37, 38]. The molar absorptivity (ϵ) values of the prepared complexes with the metal ions under investigation were determined using 1.0×10^{-3} M DMSO solution of the synthesized complexes, by using the relation: $A = \epsilon cl$, where, A = absorbance, $c = 1.0 \times 10^{-3}$ M, l = length of cell (1 cm).

Table 3. UV-Vis spectra of HL and its metal complexes.

Compounds	Ligand transitions ($n \rightarrow \pi^*$ and $\pi \rightarrow \pi^*$) max (nm)	Ligand-metal Charge transfer max (nm)	ϵ ($M^{-1} cm^{-1}$)	d-d transition max (nm)	ϵ ($M^{-1} cm^{-1}$)
HL	275, 284, 318	-	-	-	-
(A)	275, 284, 317	572	375	609	275
(B)	275, 284, 311, 360	563	167	618	333
(C)	275, 284, 318	500	111	-	-
(D)	286, 359	527	3500	-	-
(E)	275, 284, 318	509	313	-	-
(F)	246, 320	536	73	-	-

Table 4. 1H NMR values (ppm) and tentative assignments for HL and its metal complexes.

HL	11.25	10.87	7.22–8.23	6.85–6.89		2.51	1.22
(A)	11.09	10.72	7.07–7.311	6.70–6.74	3.99–4.10	2.50	1.08
(B)	11.25	10.87	7.45	6.87	3.31–4.15	2.501	1.5
(C)	11.42	10.89	7.26–8.25	6.84–6.91	3.34–4.19	2.51	1.22
(D)	11.49	10.20	7.24–8.99	6.87–6.91	3.33	2.99	1.05
(E)	11.42	10.88	7.21–7.46	6.84–6.91	3.32–4.20	2.51	1.22
(F)	11.25	10.87	7.40–8.99	6.64–6.92	-	2.50	1.06
Complex (E) in D ₂ O	-	-	7.00–8.99	6.91	3.32–4.20	2.51	1.24
Assignments	, OH ^(s)	, -NH ^(s)	, -CH ^(m) aromatic	, -CH ^(s) HC=N	, H ₂ O	, -CH ₂	, -CH ₃

1H NMR spectra

The proton NMR spectra of the compounds were recorded in DMSO-*d*₆ as a solvent (Table 4). The 1H NMR spectrum of HL showed singlet at δ : 6.85–6.89 ppm corresponding to -CH aliphatic, multiplet at δ : 7.22–8.23 ppm for -CH aromatic, triplet at δ : 1.22 ppm corresponding to (3H, CH₃), quarter at δ : 2.51 ppm corresponding to (2H, CH₂), singlet at δ : 10.87 ppm corresponding to -NH of amide group and singlet at δ : 11.25 ppm corresponding to (H, OH). The two signals are disappeared upon addition of D₂O. Also, the 1H NMR spectra for complexes exhibit new peak in the range 3.31–4.20 ppm, due to the presence of water molecules in the complexes [39]. On comparing main peaks of free HL with its complexes, it is observed that all the peaks of the free ligand are present in the spectra of the complexes with chemical shift upon binding of free HL to the metal ion. In order to make sure for the presence of the two protons of -OH and -NH in all complexes, the spectrum of La(III) complex as an example was done in presence of D₂O which indicated the presence of -OH and -NH protons in the complex.

Mass spectra

The idea of mass spectrometer builds up on the disconnection of ion of fragments ions dependent to the variation of these ions with the ratio of mass to charge (m/z) [40]. Mass spectrum of the synthesized Schiff base is in a good agreement with the suggested structure. The electron impact spectra of the prepared complexes are recorded and inspected at 70 eV. The mass spectra of complexes (A), (B), (C), (D), (E) and (F) displayed molecular peaks at 670, 633, 645, 629, 785 and 804 which refer to M.Wt. of these complexes (Figure 1). The HL showed molecular peak (M^+) at $m/z = 208$ (79%). The molecular ion peak [a] loses C_2H_5COO to give fragment which refer to base peak [b] at $m/z = 135$ (60%). The molecular ion peak [a] loses C_6H_5O to give fragment [c] at $m/z = 115$ (73%). It loses NH to give [d] at $m/z = 193$ (85%). The molecular ion peak [a] give fragment [e] at $m/z = 180$ (50%) when loss N_2 and also loss C_2H_5 to give [f] at $m/z = 179$ (30%). The fragmentation patterns of our studied complexes were obtained from mass spectra. The mass spectrum of complex (B) displayed molecular peak at $m/z = 633$ (60%) suggesting that the molecular weight of the assigned product matching with elemental analysis calculated. Fragmentation pattern of the complex (B) is given as an example. The molecular ion peak [a] appeared at $m/z = 633$ (60%) loses 2NH to give [b] at $m/z = 603$ (50%) and it also loses $(CH_3COO)_2 \cdot 2H_2O$ to give [c] at $m/z = 479$ (45%). The molecular ion peak [a] loses NH to give [d] at $m/z = 618$ (90%) and it loses C_6H_4 to give [e] at $m/z = 557$ (85%). The molecular ion peak also loses $2C_6H_4$ to give [f] at $m/z = 481$ (40%) and also [g] at $m/z = 543$ (35%) due to loss of $2C_2H_5O$.

Thermal analyses

Thermal analysis has a main role in studying both the properties and stoichiometry of the derived volatile decomposition products, the destruction of the initial crystal lattice, the formation of crystallization centers and their growth, the thermal decomposition of one chemical bond and the formation of others, the diffusion of gases, the adsorption of gaseous products, heat transfer and many other elemental processes. To establish the proposed formulas for all compounds under investigation, thermogravimetric analyses (TG) and differential thermogravimetric (DTG) analyses were carried out, under nitrogen atmosphere and the weight loss is measured from the ambient temperature up to ~ 1000 °C. The TG and DTG curves of HL and its complexes are shown in Figure 2 and the data listed gives the maximum temperature values, $T_{max}/^{\circ}C$ together with the corresponding weight loss for each step of the decomposition reactions of the above complexes. These data support the proposed complexes chemical formulas under investigation. The data obtained indicate that the HL is thermally stable at room temperature. Decomposition of the HL started at 73 °C and finished at 800 °C with one stage at two maxima 227 and 554 °C and is accompanied by a weight loss 99.74%, corresponding exactly to the loss of $2.5C_2H_4 + 3CO + 2HCN$ which very closely to calculated value 100%. The TG curve of complex (A) shows two stages of decomposition. The first stage of decomposition occurs with two maxima 56, 119 °C and is accompanied by a weight loss of 13.80% (calcd. 13.40%), corresponding to the loss of $5H_2O$. The second stage of decomposition occurs with five maxima 207, 321, 370, 594 and 801 °C and is accompanied by a weight loss of 73.07% (calcd. 73.67%) corresponding to the loss of $4NO + 2HCl + CO + 7C_2H_2 + 2C_2H_4$, giving $CoO + C$ as a final product with weight loss of 13.16% (calcd. 12.94%). The TG curve of complex (B) exhibits three main degradation steps. The first step of decomposition occurs in the range 47-137 °C, with a maximum temperature of 103 °C and is accompanied by a weight loss of 5.68%, corresponding to the loss of $2H_2O$.

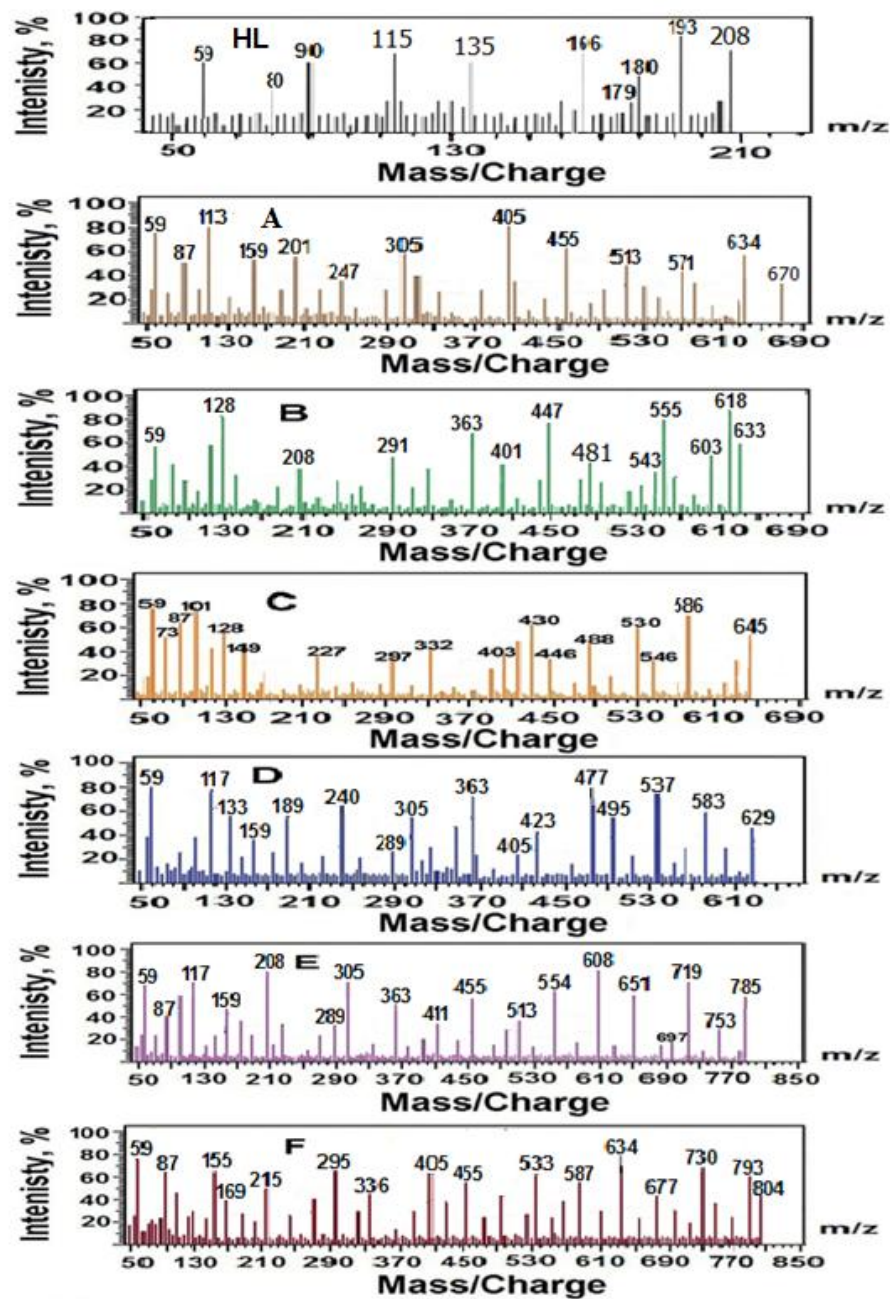


Figure 1. Mass spectra diagrams for **HL** and its metal complexes.

The second step of decomposition occurs in the range 139-401 °C, with two maxima 201 and 261 °C and is accompanied by a weight loss of 18.55 % (calcd. 18.63%), corresponding to the loss of $C_2H_6+2CO_2$. The third step of decomposition occurs in the range 402-1014 °C, with a maximum temperature of 582 °C and is accompanied by a weight loss of 53.85% (calcd. 53.66%), corresponding to the loss of $2NO+2H_2O+CO+7C_2H_2+2NH_3$ giving $CuO+5C$ as a final product with weight loss of 22.03% (calcd. 22.03%). The TG curve of complex (C) shows two main degradation steps. The first step of decomposition occurs at 50 and 104 °C and is accompanied by a weight loss of 5.38% (calcd. 5.56%), corresponding to the loss of $2H_2O$. The second step of decomposition occurs in the range 128-726 °C, with two maxima 227, 560 °C and is accompanied by a weight loss of 77.18% (calcd. 77.00%), corresponding to the loss of $0.5H_2O+4NO+3HCl+10C_2H_2$ giving $0.5Y_2O_3$ as a final product. Thermogravimetric (TG) curve for complex (D) exhibits two main degradation steps. The first step of decomposition occurs in the range 40-65 °C, with a maximum temperature at 53 °C and is accompanied by a weight loss of 2.86% correspond to loss of H_2O . The second step of decomposition occurs at two maxima 180 and 460 °C and is accompanied by a weight loss of 62.66% (calcd. 62.36%), corresponding to the loss of $2HCl+6C_2H_4+4NO+O_2$ giving ZrO_2+8C as a final solid product and is accompanied by a weight loss of 35.00% (calcd. 34.78%). The TG curve of complex (E) shows two steps of decomposition. The first step of decomposition occurs in the range 35-134 °C with two maximum temperature 51 and 114 °C and is accompanied by a weight loss of 11.72% (calcd. 11.43%), corresponding to the loss of $5H_2O$. The second step of 135-579 °C, with two maxima 220 and 503 °C and is accompanied by a weight loss of 64.88% (calcd. 64.83%), corresponding to the loss of $0.5H_2O+7C_2H_2+4NO+Cl_2O+3CH_4+CO+HCl$ giving $0.5La_2O_3+2C$ as a final product. The TG curve of complex (F) exhibits two main degradation steps. The first step of decomposition occurs in the range 39-276 °C, with a maximum temperature of 257 °C and is accompanied by a weight loss of 14.68%, corresponding to the loss of $C_2H_6+2CO_2$. The second step of decomposition occurs in the range 277-589 °C, with two maxima 355 and 458 °C and is accompanied by a weight loss of 33.92% (calcd. 33.83%), corresponding to the loss of $4C_2H_6+2NO+2NO_2$ giving UO_2+12C as a final product. The decomposition mechanisms are only based on speculation and the thermal analysis without a complementary technique (gas chromatography). The suggested residues confirmed only on the basis weight loss % calculation and infrared spectra.

The kinetic studies

There has been increasing advantage in determining rate-dependent parameters of solid-state non-isothermal decomposition reactions by analysis of TGC. Several equations have been proposed to analyze TGC and obtained values for kinetic parameters [41]. The kinetic parameters have been evaluated using the following methods [42, 43] and the results obtained by these methods are compared with one another. The following two methods are briefly discussed.

Coats-Redfern equation [42]

The *Coats-Redfern* equation (1), which is a typical integral method, can be represented as:

$$\int_0^\alpha \frac{d\alpha}{(1-\alpha)^n} = - \int_{T_i}^{T_f} \exp\left(\frac{-E^*}{RT}\right) dT \quad (4)$$

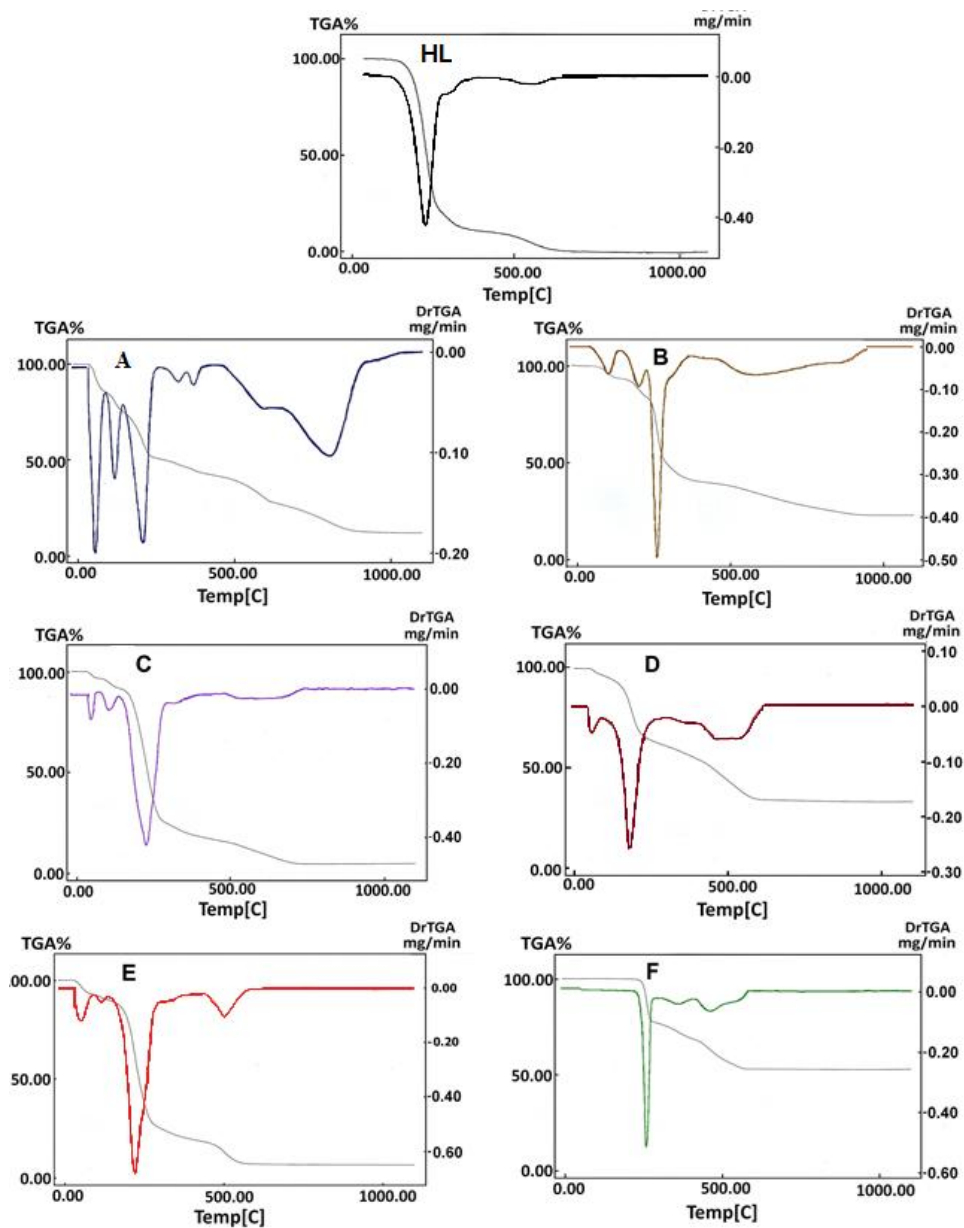


Figure 2. TG and DTG diagrams for *HL* and its metal complexes.

For convenience of integration, the lower limit T_l is usually taken as zero. equation on integration gives:

$$\ln X = \ln \left[\frac{-\ln(1-\alpha)^{1-n}}{T^2(1-n)} \right] = \frac{-E^*}{RT} + \ln \left[\frac{AR}{\varphi E^*} \right] \text{ for } n \neq 1 \quad (5)$$

$$\ln X = \ln \left[\frac{-\ln(1-\alpha)}{T^2} \right] = \frac{-E^*}{RT} + \ln \left[\frac{AR}{\varphi E^*} \right] \text{ for } n = 1 \quad (6)$$

where β is the linear heating rate dT/dt , R is the gas constant in $J K^{-1} mol^{-1}$ and α is the fraction decomposed at time t . The correlation coefficient, r , was computed using the least squares method for different values of n ($n = 0, 0.33, 0.5, 0.66$ and 1) by plotting $\ln X$ versus $1/T$ for the investigated metal complexes. E^* is the energy of activation in $kJ mol^{-1}$ and calculated from the slope and A in (s^{-1}) from the intercept. The entropy of activation ΔS^* in ($kJ/mol.K$) was calculated by using equation (4):

$$\Delta S^* = R \ln \left(\frac{Ah}{K_B T_s} \right) \quad (7)$$

where K_B is the Boltzmann constant, h is the Plank's constant and T_s is the DTG peak temperature.

Horowitz-Metzger equation [43]

The *Horowitz-Metzger* equation is an illustrative of the approximation methods. These authors derived the relation:

$$\ln[-\ln(1-\alpha)] = \frac{E_a \theta}{RT_s^2} \quad \text{for } n=1 \quad (8)$$

$$\ln \left[\frac{\{1-(1-\alpha)^{1-n}\}}{(1-n)} \right] = \ln \left(\frac{AR T_s^2}{\Phi E} \right) - \frac{E_a}{RT_s} + \frac{E_a \theta}{RT_s^2} \quad \text{for } n \neq 1 \quad (9)$$

where $\theta = T - T_s$, T_s is the DTG peak temperature, T the temperature corresponding to weight loss. In this method a straight line should be observed between the left hand sides of equations (5) and (6) versus θ with a slope of E_a/RT_s^2 . The entropy of activation, ΔS^* , the enthalpy of activation, ΔH^* and Gibbs free energy, ΔG^* , were calculated from;

$$\Delta H^* = E^* - RT \quad (10) \text{ and } \Delta G^* = \Delta H^* - T \Delta S^* \quad (11)$$

All decomposition steps show the best fit for $n = 1$. The negative value of the entropy of activation, ΔS^* of some decomposition steps indicates that the activated fragments have more ordered structure than the undecomposed ones and the later are slower than the normal [44, 45]. The positive sign of activation enthalpy change, ΔH^* indicates that the decomposition stages are endothermic processes [46]. The high values E^* (Table 5) reveals the high stability of such chelates due to their covalent bond character. The increase of E^* for complex (F) reflects the greater thermal stability of the complex than the other complexes and the processes involving in translational, rotational, vibrational states and a changes in mechanical potential energy for complexes [47]. The positive sign of ΔG^* reveals that the free energy of the final residue is

higher than that of the initial compound, and hence all the decomposition steps are non-spontaneous processes.

Table 5. Thermal behavior and kinetic parameters determined using the Coats–Redfern (CR) and Horowitz–Metzger (HM) operated for **HL** and its metal complexes.

Compounds	Decomposition range (K)	T _s (K)	Method	Parameters					R ^a	SD ^b
				E [‡] (kJ/mol)	A (s ⁻¹)	S [‡] (kJ/mol.K)	H [‡] (kJ/mol)	G* (kJ/mol)		
HL	100-650	500	CR	83.76	2.40×10 ⁶	-0.1203	79.60	139.77	0.997	0.08
			HM	101.53	3.30×10 ⁸	-0.0861	97.38	140.44	0.998	0.07
(A)	307-366	329	CR	53.26	1.14×10 ⁶	-0.1297	50.52	93.21	0.999	0.03
			HM	55.33	2.39×10 ⁵	-0.1156	52.59	90.64	0.998	0.81
	421-528	480	CR	104.45	4.12×10 ⁹	-0.0648	100.46	131.58	0.990	0.13
			HM	120.99	1.55×10 ¹¹	-0.0347	116.99	133.64	0.990	0.15
(B)	320-410	534	CR	91.83	3.65×10 ⁶	-0.1241	87.39	153.67	0.999	0.03
			HM	97.87	2.58×10 ⁷	-0.1079	93.43	151.03	0.999	0.03
(C)	401-551	500	CR	46.90	3.35×10 ²	-0.2009	42.74	143.17	0.995	0.07
			HM	58.43	5.95×10 ³	-0.1769	54.27	142.74	0.995	0.09
(D)	313-338	453	CR	45.24	5.30×10 ²	-0.1962	41.47	130.37	0.999	0.05
			HM	57.15	2.18×10 ⁴	-0.1653	53.39	128.29	0.990	0.18
(E)	408-551	493	CR	40.76	3.41×10 ²	-0.2198	36.65	145.21	0.990	0.08
			HM	47.80	4.43×10 ²	-0.1984	43.69	141.72	0.990	0.11
(F)	312-549	530	CR	129.41	3.07×10 ¹⁰	-0.0489	125.00	150.94	0.980	0.17
			HM	137.32	3.35×10 ¹¹	-0.0290	132.92	148.31	0.980	0.20

X-ray powder diffraction

The powder XRD patterns of HL and complexes [(**A**), (**B**), (**C**), (**D**), (**E**) and (**F**)] were recorded over 2 θ in the range scale (10-70). The diffraction of HL, shows four sharp diffraction peaks at about 2 θ [d value Å] = 11.24[7.87], 18.23[4.87], 24.01[3.71] and 25.97[3.43]. The diffractogram of complex (**A**), indicated main peaks at 2 θ [d value Å] = 8.33[10.61], 15.75[5.63], 16.11[5.50], 18.47[4.80], 19.46[4.55], 22.86[3.89], 25.26[3.53], 26.17[3.41], 29.87[2.99], 30.25[2.93], 32.48[2.76], 33.04[2.71], 34.95[2.57], 37.37[2.41], 40.92[2.21], 45.71[1.98] and 47.83[1.90]. The XRD patterns of complex (**B**), exhibited sharp peaks corresponding to 2 θ [d value Å] = 6.51[13.57], 9.02[9.80], 10.37[8.53], 11.52[7.68], 14.34[6.18], 23.42[3.80], 24.90[3.58], 25.93[3.44] and 28.32[3.15]. The X-ray powder diffraction for complex (**C**), give five sharp peaks at 2 θ [d value Å] = 8.31[10.46], 11.20[7.90], 18.21[4.87], 23.97[3.71] and 25.91[3.44]. The diffraction of complex (**D**), give six sharp peaks at 2 θ [d value Å] = 8.31[10.64], 15.26[5.80], 22.83[3.90], 26.16[3.41], 26.75[3.33] and 32.66[2.74]. The XRD patterns of complex (**E**), give three peaks at 2 θ [d value Å] = 8.32[10.63], 16.65[5.33] and 26.14[3.41]. The XRD patterns of complex (**F**), give peaks at 2 θ [d value Å] = 7.83[11.30], 11.26[7.86], 13.67[6.48], 21.25[4.18], 22.67[3.92], 24.06[3.70] and 26.34[3.38]. The mean crystallite sizes, estimated using Scherer equation [48], are shown in Table 6. The data in this table clarify that, the HL and its metal complexes display crystalline peaks.

$$t = \frac{K\lambda}{\beta \cos\theta} \quad (12)$$

t is the mean size of the ordered (crystalline) domains, which may be smaller or equal to the grain size, which may be smaller or equal to the particle size. K is a dimensionless shape factor,

with a value close to unity. The shape factor has a typical value of about 0.9, but varies with the actual shape of the crystallite. λ is the X-ray wavelength. $\Delta 2\theta$ is the line broadening at half the maximum intensity (FWHM), after subtracting the instrumental line broadening, in radians. This quantity is also sometimes denoted as $(\Delta 2\theta)$. θ is the Bragg angle.

Table 6. The average crystallite size of HL and its complexes estimated from XRD pattern.

Compounds	2θ ($^\circ$)	d value (Å)	Relative intensity (%)	Full width at half maximum (FWHM) ^a	Average crystallite size (nm)
HL	25.97	3.43	100	0.22	37.46
(A)	18.47	4.80	100	0.20	40.15
(B)	11.52	7.68	100	0.22	36.68
(C)	25.91	3.44	100	0.22	37.06
(D)	32.66	2.74	100	0.20	41.29
(E)	8.32	10.63	100	0.20	39.84
(F)	7.83	11.30	100	0.20	39.83

^aThe maximum diffraction patterns according to the highest value of intensity.

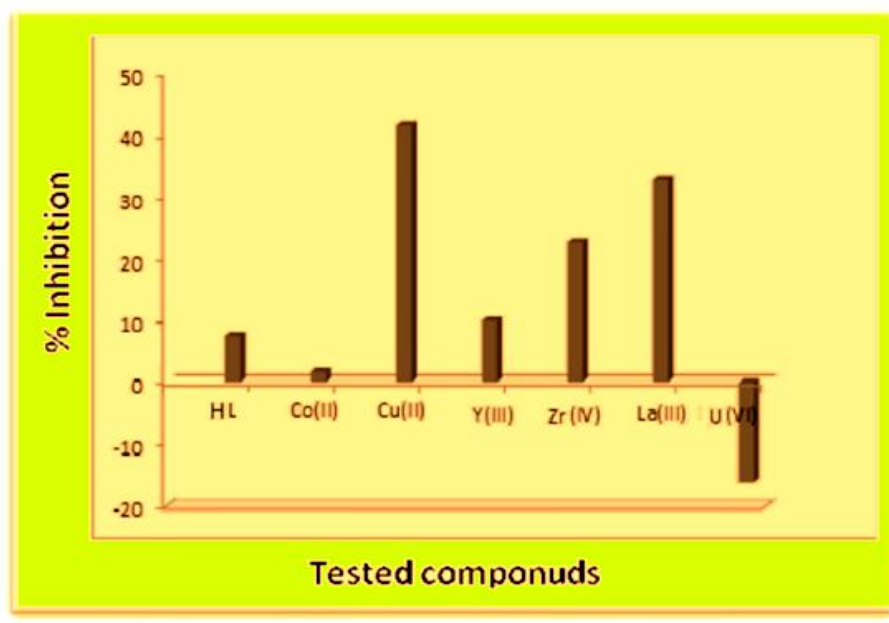


Figure 3. Effect of **HL** and its metal complexes with 5000 mg/L against migration of second stage larvae of root-knot nematode *Meloidogyne javanica* under laboratory conditions.

Biological activity

The preliminary screening of HL and its complexes was evaluated with 5000 mg/L on migration of second stage larvae of root not nematode *Medoiolgyne javanica* under laboratory conditions (Figure 3). The nematicidal activity of tested complexes except (**F**) showed the descending order was (**B**), (**E**), (**D**), (**C**) and (**A**). The inhibition percentages were 41.70, 32.90, 22.70, 10.00 and 0.00, respectively, on contrast complex (**F**) stimulated migration of tested nematode compared with **HL**.

CONCLUSIONS

Metal complexes of Co(II), Cu(II), Y(III), Zr(IV), La(III) and U(VI) with Schiff base ligand were formed in 1:1 molar ratio and then characterized by various physicochemical and spectroscopic techniques. The spectroscopic data showed that the HL ligand acted as tetradentate ligand and it coordinated to metal ions through oxygen of phenolic group and nitrogen atom in C=N group. All the prepared complexes had octahedral structures. The stability of the complexes was explained and kinetic parameters (E_a , H, S, G) of the thermal decomposition stages have been evaluated using the Coats–Redfern and Horowitz–Metzger methods. The nematicidal effect of complex (B) changed to stimulation effect in case of complex (F) that increased migration of nematode.

REFERENCES

1. Castagnone-Sereno, P. Genetic variability in parthenogenetic root-knot nematodes, *Meloidogyne spp.*, and their ability to overcome plant resistance genes. *Nematologica* **2002**, 4, 605-608.
2. Karuri, H.W.; Olago, D.; Neilson, R.; Mararo, E.; Villinger, J. A survey of root knot nematodes and resistance to *Meloidogyne incognita* in sweet potato varieties from Kenyan fields. *Crop Protection* **2017**, 92, 114-121.
3. El-Kady, A.M.A.; Hamouda, S.E.S.; Ibrahim, H.S.; Abd-Alla, H.I. Formulating salicylic acid as (emulsifiable concentrate, wettable granule) and study their nematicidal efficiency on root-knot nematode. *J. Amer. Sci.* **2014**, 10, 146-153.
4. Korayem, A.M.; Youssef, M.M.A.; Mohamed, M.M.M.; Lashein, A.M.S. Plant-parasitic nematodes associated with different plants grown in newly reclaimed area in North West Egypt. *Egypt. J. Agronematol.* **2015**, 14, 127-136.
5. Abd El-Hamid, S.M.; Sadeek, S.A.; El-Farargy, A.F.; Abd El-Latif, N.S. Synthesis, structural characterization and nematicidal studies of some new N₂O₂ Schiff base metal complexes. *Bull. Chem. Soc. Ethiop.* **2021**, 35(2), in press.
6. Zukerman, B.M.; Esnard, J. Biological control of plant nematodes-current status and hypotheses. *Jpn. J. Nematol.* **1994**, 24, 1-13.
7. Al-Hazmi, A.S.; Dawabah, A.A.M.; Al-Nadhari, S.N.; Al-Yahya, F.A. Comparative efficacy of different approaches to managing *Meloidogyne incognita* on green bean. *Saudi J. Biol. Sci.* **2017**, 24, 149-154.
8. Ispir, E.; Kurtoglu, M.; Toroglu, S. The d¹⁰ metal chelates derived from schiff base ligands having silane: synthesis, characterization, and antimicrobial studies of cadmium(II) and zinc(II) complexes. *Inorg. Met. Org. Nano-Met. Chem.* **2006**, 36, 627-631.
9. Uddin, S.; Hossain, Md.S.; Latif Md.A.; Karim, Md.R.; Mohapatra, R.K.; Zahan, Md.K. E. Antimicrobial activity of Mn complexes incorporating Schiff bases: A short review. *Amer. J. Heter. Chem.* **2019**, 5, 27-36.
10. Da Silva, C.M.; Da Silva, D.L.; Modolo, L.V.; Alves, R.B.; De Resende, M.A.; Martins C.V.B.; Fátima, Â. Schiff bases: A short review of their antimicrobial activities. *J. Adv. Res.* **2011**, 2, 1-8.
11. Fátimaa, Â.; Pereira, C.P.; Dau Gonçalves Olímpioa, C.R.S.; Oliveiraa, B.G.F.; Francoab, L.L.; Silvaa, P.H.C. Schiff bases and their metal complexes as urease inhibitors – A brief review. *J. Adv. Res.* **2018**, 13, 113-126.
12. El-Behery, M.; El-Twigry, H. Synthesis, magnetic, spectral, and antimicrobial studies of Cu(II), Ni(II) Co(II), Fe(III), and UO₂(II) complexes of a new Schiff base hydrazone derived from 7-chloro-4-hydrazinoquinoline *Spectrochim. Acta A* **2007**, 66, 28-36.

13. El-Kholy, N.G. Study of the ternary complexes of Fe(III) and UO₂(II) with *o*-tolidine derivatives with 2-aminopyridine and oxalic acid in the solid state. *Life Sci. J.* **2014**, 11, 790-817.
14. Kavitha, P.; Chary, M.R.; Singavarapu, B.V.V.A.; Reddy, K.L. Synthesis, characterization, biological activity and DNA cleavage studies of tridentate Schiff bases and their Co(II) complexes. *J. Saudi Chem. Soc.* **2016**, 20, 69-80.
15. Ahmed, F.M.; Sadeek, S.A.; El-Shwiniy, W.H. Synthesis, spectroscopic studies, and biological activity of some new N₂O₂ tetradentate Schiff base metal complexes. *Russ. J. Gen. Chem.* **2019**, 89, 1874-1883.
16. Sadeek, S.A.; Mohamed, A.A.; El Sayed, H.A.; El Attar, M.S. Spectroscopic characterization, thermogravimetric and antimicrobial studies of some new metal complexes derived from 4-(4-isopropyl phenyl)-2-oxo-6-phenyl 1,2-dihydropyridine-3-carbonitrile (L). *App. Organomet. Chem.* **2020**, 34, e5334.
17. El-Attar, M.S.; Abd El-Lattif, N.S.; Sadeek, S.A. Study on the nematicidal activity and chemical structure of NO bidentate Schiff base some metal complexes. *J. Chin. Chem. Soc.* **2020**, 67, 610-622.
18. Addabbo, T.D.; Argentieri, M.P.; uchowski, J.; Biazzzi, E.; Tava, A.; Oleszek, W.; Avato, P. Activity of saponins from *Medicago species* against phytoparasitic nematodes. *Plants* **2020**, 9, 443.
19. Seco, J.M.; Quiros, M.; Garmendia, M.J. Synthesis, X-ray crystal structure and spectroscopic, magnetic and EPR studies of copper(II) dimers with methoxy-di-(2-pyridyl)methoxide as bridging ligand. *Polyhedron* **2000**, 19, 1005-1013.
20. Sadeek, S.A.; Abd El-Hamid, S.M.; Rashid, N.G. Spectroscopic characterization and XRD of some new metal complexes with dithranol in presence of 8-hydroxyquinoline. *Egypt. J. Chem.* **2020**, 63, 939-951.
21. Jouad, E.M.; Riou, A.; Allain, M.; Khan, M.A.; Bouet, G.M. Synthesis, structural and spectral studies of 5-methyl-2-furaldehyde thiosemicarbazone and its Co, Ni, Cu and Cd complexes. *Polyhedron* **2001**, 20, 67-74.
22. Rodney, P.F.; Nakayama-Ratchford, N.; Dai, H.; Lippard, S.J. Soluble single-walled carbon nanotubes as longboat delivery systems for platinum(IV) anticancer drug design. *J. Am. Chem. Soc.* **2007**, 129, 8438-8439.
23. Philip, V.; Suni, V.; Kurup, M.R.P.; Nethaji, M. Copper(II) complexes derived from di-2-pyridyl ketone N(4),N(4)-(butane-1,4-diyl)thiosemicarbazone: Crystal structure and spectral studies. *Polyhedron* **2006**, 25, 1931-1938.
24. Kim, G.W.; Koo, B.K. Synthesis and crystal structures of cadmium(II) complexes with 2-acetylpyridine Schiff bases of S-methyldithiocarbazate or 4-phenyl 3-thiosemicarbazide. *J. Kor. Chem. Soc.* **2019**, 63, 392-397.
25. Al-Shihri, S.A. Synthesis, characterization and thermal analysis of some new transition metal complexes of a polydentate Schiff base. *Spectrochim. Acta A* **2004**, 60, 1189-1192.
26. Mohamed, G.G.; Abd El-Wahab, Z.H. Mixed ligand complexes of bis(phenylimine) Schiff base ligands incorporating pyridinium moiety: Synthesis, characterization and antibacterial activity. *Spectrochim. Acta A* **2005**, 61, 1059-1068.
27. El-Shafiey, Z.A. Synthesis, spectroscopic characterization, thermal investigation and antimicrobial activity of S, O and N-donor heterocyclic Schiff base ligands and their Co(II), Cd(II), Hg(II), Fe(III) and UO₂(II) metal complexes. *Egypt. J. Chem.* **2010**, 53, 137-162.
28. Wang, G.; Chang, J.C. Synthesis and characterization of amino acid Schiff base complexes of nickel(II). *Synth. React. Inorg. Met-Org. Chem.* **1994**, 24, 1091-1097.
29. Abd El Hamid, S.M.; Sadeek, S.A.; Abd El Lattif, N.S. Study of the chemical structure and their nematicidal activity of N₂O₂ tetradentate Schiff base metal complexes. *App. Org. Chem.* **2019**, 33, e5010.

30. Nour, E.M.; AL-Kority, A.M.; Sadeek, S.A.; Teleb, S.M. Synthesis and spectroscopic studies of NN-O-phenylenebis (salicylideneiminato) dioxouranium (VI) solvates (L) CL = DMF and PY). *Synth. React. Inorg. Met. Org. Chem.* **1993**, 23, 39-52.
31. Zhong, D.; Chen, Z.; Liu, Y.; Luo, X.; Barta, C.; Liang, H. Syntheses, crystal structures of Ni(II), Ag(I)-enoxacin complexes, and their antibacterial activity. *J. Coord. Chem.* **2010**, 63, 3146-3154.
32. Mcglynn, S.P.; Smith, J.K. The electronic structure, spectra, and magnetic properties of actinyl ions: Part I. The uranyl ion. *J. Mol. Spect.* **1961**, 6, 164-187.
33. Jones, L.H. Determination of U-O bond distance in uranyl complexes from their infrared spectra. *Spectrochim. Acta A* **1959**, 11, 409-411.
34. Beiswenger, T.N.; Gallagher, N.B.; Myers, T.L.; Szecsody, J.E.; Tonkyn, R.G.; Su, Y.F.; Sweet, L.E.; Lewallen, T.A.; Johnson, T.J. Identification of uranium minerals in natural U-bearing rocks using infrared reflectance spectroscopy. *App. Spect.* **2018**, 72, 209-224.
35. Lever, A.B.P. The electronic spectra of tetragonal metal complexes analysis and significance. *Coord. Chem. Rev.* **1968**, 3, 119-140.
36. Sadeek, S.A.; Mohamed, A.A.; Zordok, W.A.; Awad, H.M.; Abd El-Hamid, S.M. Spectroscopic characterization, thermogravimetric, DFT and biological studies of some transition metals complexes with mixed ligands of meloxicam and 1,10-phenanthroline. *Egypt. J. Chem.* **2021**, 64, 4197-4208.
37. Mondal, N.; Dey, D.K.; Mitra, S.; Malik, K.M.A. Synthesis and structural characterization of mixed ligand 1-2-hydroxyacetophenone complexes of cobalt(III). *Polyhedron* **2000**, 19, 2707-2711.
38. Sadeek, S.A.; El-Attar, M.S.; Abd El-Hamid, S.M. Synthesis and characterization and antibacterial activity of some new transition metal complexes with ciprofloxacin-imine. *Bull. Chem. Soc. Ethiop.* **2015**, 29, 259-274.
39. Sadeek S.A.; Refat M.S.; Teleb S.M.; El-Megharbel S.M. Synthesis and characterization of V(III), Cr(III) and Fe(III) hippurates. *Mol. Struct.* **2005**, 737, 139-145.
40. Sanmartin, J.; Novio, F.; Garcia-Deibe, A.M.; Fondo, M., Ocampo, N.; Bermejo, M.R. Dinuclear neutral complexes of a symmetric N₂ + N₂-donor diimine ligand. *Polyhedron* **2006**, 25, 1714-1722.
41. Sestak, J.; Satava, V.; Wendlandt, W.W. The study of heterogeneous processes by thermal analysis. *Thermochim. Acta* **1973**, 7, 333-336.
42. Coats, A.W.; Redfern, J.P. Kinetic parameters from thermogravimetric data. *Nature* **1964**, 201, 68-69.
43. Horowitz, H.H.; Metzger G. A new analysis of thermogravimetric traces. *Anal. Chem.* **1963**, 35, 1464-1468.
44. Nirmal, R.; Prakesh, C.R.; Menakshi, K.; Shanmugapandiyam, P. Synthesis pharmacological evaluation of novel Schiff base analogues of 3-(4-amino) phenylimino) 5-fluorindolin-2-one. *J. Young Pharm.* **2010**, 2, 162-168.
45. Mondol, P.; Banerjee, M.; Jana, S.; Bose, A. Synthesis and evaluation of 1,3 di-substituted Schiff, Mannich bases and spiro isatin derivatives. *J. Young Pharm.* **2010**, 2, 169-172.
46. El-Megharbel, S.M.; Hamza, R.Z.; Refat, M.S. Synthesis, chemical identification, antioxidant capacities and immunological evaluation studies of a novel silver(I) carbocysteine complex. *Chem. Biol. Interact.* **2014**, 220, 169-180.
47. Harris, G.M. Kinetics and mechanism (Eds. Frost, A.A.; Pearson, R.G.). *Inorg. Chem.* **1963**, 2, 432.
48. Quan, C.X.; Bin, L.H.; Bang, G.G. Preparation of nanometer crystalline TiO₂ with high photo-catalytic activity by pyrolysis of titanil organic compounds and photo-catalytic mechanism. *Mat. Chem. Phys.* **2005**, 91, 317-324.